Light: Science & Applications (2017) 6, e17021; doi:10.1038/lsa.2017.21
Official journal of the CIOMP 2047-7538/17
www.nature.com/lsa

ORIGINAL ARTICLE

Few-mode fibre-optic microwave photonic links

He Wen[1,2], Hongjun Zheng[1,3], Qi Mo[4], Amado Manuel Velázquez-Benítez[1], Cen Xia[1], Bin Huang[1], Huiyuan Liu[1], Huang Yu[4], Pierre Sillard[5], Jose Enrique Antonio Lopez[1], Rodrigo Amezcua Correa[1] and Guifang Li[1,2]

The fibre-optic microwave photonic link has become one of the basic building blocks for microwave photonics. Increasing the optical power at the receiver is the best way to improve all link performance metrics including gain, noise figure and dynamic range. Even though lasers can produce and photodetectors can receive optical powers on the order of a Watt or more, the power-handling capability of optical fibres is orders-of-magnitude lower. In this paper, we propose and demonstrate the use of few-mode fibres to bridge this power-handling gap, exploiting their unique features of small acousto-optic effective area, large effective areas of optical modes, as well as orthogonality and walk-off among spatial modes. Using specially designed few-mode fibres, we demonstrate order-of-magnitude improvements in link performances for single-channel and multiplexed transmission. This work represents the first step in few-mode microwave photonics. The spatial degrees of freedom can also offer other functionalities such as large, tunable delays based on modal dispersion and wavelength-independent lossless signal combining, which are indispensable in microwave photonics.
Light: Science & Applications (2017) **6,** e17021; doi:10.1038/lsa.2017.21; published online 11 August 2017

Keywords: analogue optic-fibre link; few-mode fibre; fibre nonlinearity; microwave photonics; space-division multiplexing

INTRODUCTION

Optical fibre has long been recognized as a superior medium for transmission of radio-frequency (RF) and microwave signals due to its low loss, large bandwidth, light weight and immunity to electromagnetic interference[1–4]. The ability to simultaneously achieve high gain, low noise figure and large spurious-free dynamic range (SFDR) determines the roles fibre-optic microwave photonic links can play in many microwave photonics applications. Much research effort has been devoted to achieving this goal, including high-power lasers[5,6], linear, efficient and low-loss modulators[7–9], and photodetectors with high quantum efficiency and power-handling capability[10,11]. These efforts have enabled high-performance fibre-optic microwave photonic links[12–14]. Yet, so far the composite performance of a fibre-optic microwave photonic link realized using a low-loss optical fibre cannot compete with that using a high-loss microwave cable and a high-performance electronic amplifier.

It is well recognized that increasing the optical power before photodetection is the most effective way to simultaneously achieve high gain, low noise figure and large dynamic range[15–18]. A 1-dB increase in the received optical power leads to a 2-dB increase in the detected microwave power, a 2-dB increase in thermal noise-dominated signal-to-noise ratio (SNR), and a 4/3-dB increase in SFDR[15–18]. For reference, to achieve lossless transmission (0 dB microwave power gain) over a 20 km intensity-modulation direct-detection (IM-DD) fibre-optic microwave photonic link, the required input optical power is 63 mW or 18 dBm using a Mach–Zehnder modulator with a half-wave voltage of 4 V and an ideal photodiode[15]. This power-handling ability is well within the capabilities of the state-of-the-art optoelectronic components. Single-mode semiconductor lasers can produce optical power well over 40 dBm (Ref. 6). A travelling-wave photodiode with a maximum input power of over 25 dBm has also been demonstrated[11]. In comparison, the power-handling capability of optical fibres is orders-of-magnitude lower because of two dominant nonlinear effects in optical fibres, namely, stimulated Brillouin scattering (SBS)[19,20] and Kerr nonlinearity[21–23]. SBS results in strong backscattering that limits optical power available at the receiver, and degrades the SNR by introducing relative intensity noise due to multi-path interference[24–26]. The SBS threshold for a 20-km-long single-mode fibre (SMF) is only ~ 10 dBm (Ref. 27). Kerr nonlinearity results in self-phase modulation (SPM)[21], cross-phase modulation[28] and four-wave mixing (FWM)[22] that leads to intermodulation distortions for single-channel transmission and nonlinear crosstalk for wavelength-division multiplexed (WDM) transmission[23]. For a 20-km standard SMF, a 1.0 radian SPM is induced for an input power of only 50 mW. Applications that require fibre-optic microwave photonic links of such lengths can be

[1]CREOL, The College of Optics and Photonics, University of Central Florida, Orlando, FL 32816, USA; [2]The College of Precision Instruments and Opto-Electronics Engineering, Tianjin University, Tianjin 300072, China; [3]School of Physics Science and Information Technology, Shandong Provincial Key Lab of Optical Communication Science and Technology, Liaocheng University, Shandong 252059, China; [4]State Key Laboratory of Optical Communication Technologies and Networks, FiberHome Telecommunication Technologies Co., Ltd, Wuhan Research Institute of Posts and Telecommunications, No. 88 Youkeyuan Road, Hongshan District, Wuhan 430074, China and [5]Prysmian Group, Parc des Industries Artois Flandres, Haisnes 62092, France
Correspondence: GF Li, Email: li@creol.ucf.edu; RA Correa, Email: r.amezcua@creol.ucf.edu
Received 26 October 2016; revised 16 February 2017; accepted 19 February 2017; accepted article preview online 21 February 2017

classified into two categories[18]: microwave signal distribution (antenna remoting and phased array[29]) and microwave signal processing[1]. In antenna remoting for radio astronomy, the link lengths can be greater than 20 km (Ref. 30). Other applications that require simultaneous transmission of multiple microwave signals using WDM include phased-array antennas[31,32] and microwave photonic transversal filters[33,34]. For phased-array antennas, for example, the required SMF length for a 1-ns relative delay between antenna elements carried on WDM channels with spacing of 100 GHz is about 37 km.

Therefore, the bottleneck in improving the performance of fibre-optic microwave photonic links is the optical fibre itself. Yet there has been no concerted effort in improving the power-handling capability of optical fibres for such applications thus far. Optically preamplified links can use lower input powers and thus alleviate fibre nonlinearity but suffer SNR penalties (see detailed comparison in section 1 of Supplementary Information). Electrically amplifying input microwave signals does improve link gain, but it significantly deteriorates the SFDR due to nonlinear distortion in modulators[15]. Therefore, it is imperative to break the nonlinearity bottleneck of SMFs. We propose the use of few-mode fibres (FMF) to alleviate this bottleneck for long-haul (on the order of several kilometers) microwave photonic links[35,36]. We specifically designed and fabricated FMFs for single-channel and WDM transmission of microwave signals. First, using a 20-km FMF with a small acousto-optic effective area and a large effective area of a high-order optical mode to overcome single-channel nonlinear limitations[37], we increased the SBS threshold by 8.7 dB and the SFDR by 9.6 dB for single-channel analogue transmission as compared to that of a SMF of the same effective length. Second, by introducing FMFs into fibre-optic microwave photonic links, spatial orthogonality and phase walk-off among spatial modes can be exploited to suppress inter-channel nonlinear effects for WDM analogue transmission[38]. Using another 20-km FMF, we achieved a 30-dB reduction in nonlinear crosstalk, equivalent to a 20-dB increase in SFDR using mode-diversity WDM transmission. These demonstrations, together with recent advances in few-mode devices, can potentially usher in a new field of research, namely, few-mode microwave photonics.

MATERIALS AND METHODS

Single-channel microwave signal transmission in FMFs

FMFs can increase the nonlinear tolerance and thus optical power delivered to the photodetector for single-channel analogue transmission. Figure 1 shows the experimental setup for single-channel microwave transmission. A light wave emitted by a laser diode was modulated by two tones (1.893 and 2 GHz) using a Mach–Zehnder modulator (MZM), facilitating the standard two-tone test[15,17,39] for microwave photonic links that typically carry high carrier-to-noise ratio signals[40,41]. The MZM was low biased to suppress the optical carrier[42]. The modulated light wave was amplified, filtered and launched into a 20-km long specially designed FMF fibre via an optical circulator, which was used to measure the back-scattered light. A mode-selective photonic lantern (MSPL)[43] was inserted between the circulator and the FMF to convert the input LP_{01} fundamental mode into a specific spatial mode supported by the FMF. Figure 1b shows the structure of the MSPL that was fabricated by adiabatically tapering six input fibres of different sizes inserted into a Fluorine-doped capillary. The cross-sectional view of the MSPL output facet is shown in Figure 1c, and the output intensity profile corresponding to each input port at near field and far field are shown in Figure 1d. The mismatch between the MSPL output and the modes supported by the FMF leads to mode crosstalk. For single-channel applications, we need at least one stable mode with a large effective area in the FMF of length (crosstalk) orders-of-magnitude larger (smaller) than for those for high-power laser applications[44]. The refractive-index profile of the specially designed FMF for this application is shown in Figure 1e. With this structure, the LP_{02} mode is the most stable mode in the FMF (see section 2 of Supplementary Information for explanation). As can be seen in Figure 1f, the impulse response (see section 3 of Supplementary Information) of the LP_{02} mode is almost void of crosstalk from other modes. The low-crosstalk nature of the LP_{02} mode is also verified by the almost ideal intensity profile at the output of the FMF, as shown in the inset. The core radius of the FMF is about 11.5 μm yielding an effective area of 270 μm^2, which is about 3.8 times (5.8 dB) larger than that of the SMF. The attenuation coefficient for the LP_{02} mode is 0.27 dB km^{-1} at 1550 nm. The received signal is detected by a free-space photodetector and evaluated by an electrical spectrum analyzer.

WDM microwave signal transmission FMFs

In WDM microwave transmission, the orthogonality and walk-off of different spatial modes in FMF can be utilized to suppress WDM crosstalk mediated by fibre nonlinearity, which entails a different fibre design compared to the single-channel case as shown below. Figure 2a shows the experimental setup. Two optical carriers with 100-GHz channel spacing were coupled into the FMF through the MSPL. Without loss of generality, we set the long-wavelength channel as the target channel, which was modulated by two tones and was always launched into the LP_{01} mode of the FMF. The co-polarized interfering channel at the shorter wavelength was modulated by a single tone and could be launched into any one of the 4 LP modes: LP_{01}, LP_{11}, LP_{21} and LP_{02}. Since the microwave signal is carried on one mode only in our approach, the transfer function of the link is similar to that of SMF links, free of multi-modal dispersion[45]. The inset illustrates how FWM involving the optical carrier in the target channel and the optical carrier and one sideband of the interfering channel generates an in-band crosstalk for the target channel. Since this nonlinear crosstalk is in-band, it cannot be removed by filtering in the optical or electrical domains. To suppress such a nonlinear crosstalk, we propose and demonstrate transmitting the two WDM channels over two different modes, exploiting spatial orthogonality and increased phase mismatch among the interacting waves in addition to a larger effective area. It is possible to satisfy the phase-matching condition for FWM between different modes with frequency detuning on the order of several THz in FMFs[46,47]. In that case, spatial orthogonality between modes will still limit the FWM efficiency. For this application, there needs to be at least two stable modes that can be transported in the FMF. This is accomplished by designing and fabricating a fibre with a large effective index difference between the fibre modes[48,49]. Figure 2b and 2c shows the cross-sectional image and measured refractive-index profile respectively. The estimated core radius is 8 μm resulting an effective area of 120 μm^2, about 1.6 times of that of the standard SMF. The attenuation coefficients range from the smallest at 0.227 dB km^{-1} for the LP_{01} mode to the largest at 0.262 dB km^{-1} for the LP_{02} mode at 1550 nm. Six mode patterns, with high purity after transmitting through the FMF, are displayed in Figure 2d. The impurities in the output mode pattern mainly come from discrete crosstalk of the MSPL. Distributed crosstalk in the FMF itself is rather low, as can be seen in the impulse response in Figure 2e. Discrete mode crosstalk of the MSPL is estimated to be less than −9 dB. As a linear crosstalk, discrete crosstalk can be filtered out in the optical domain as each mode is transmitted on a different wavelength. We employed two cascaded filters to suppress this linear interference before

 doi:10.1038/lsa.2017.21

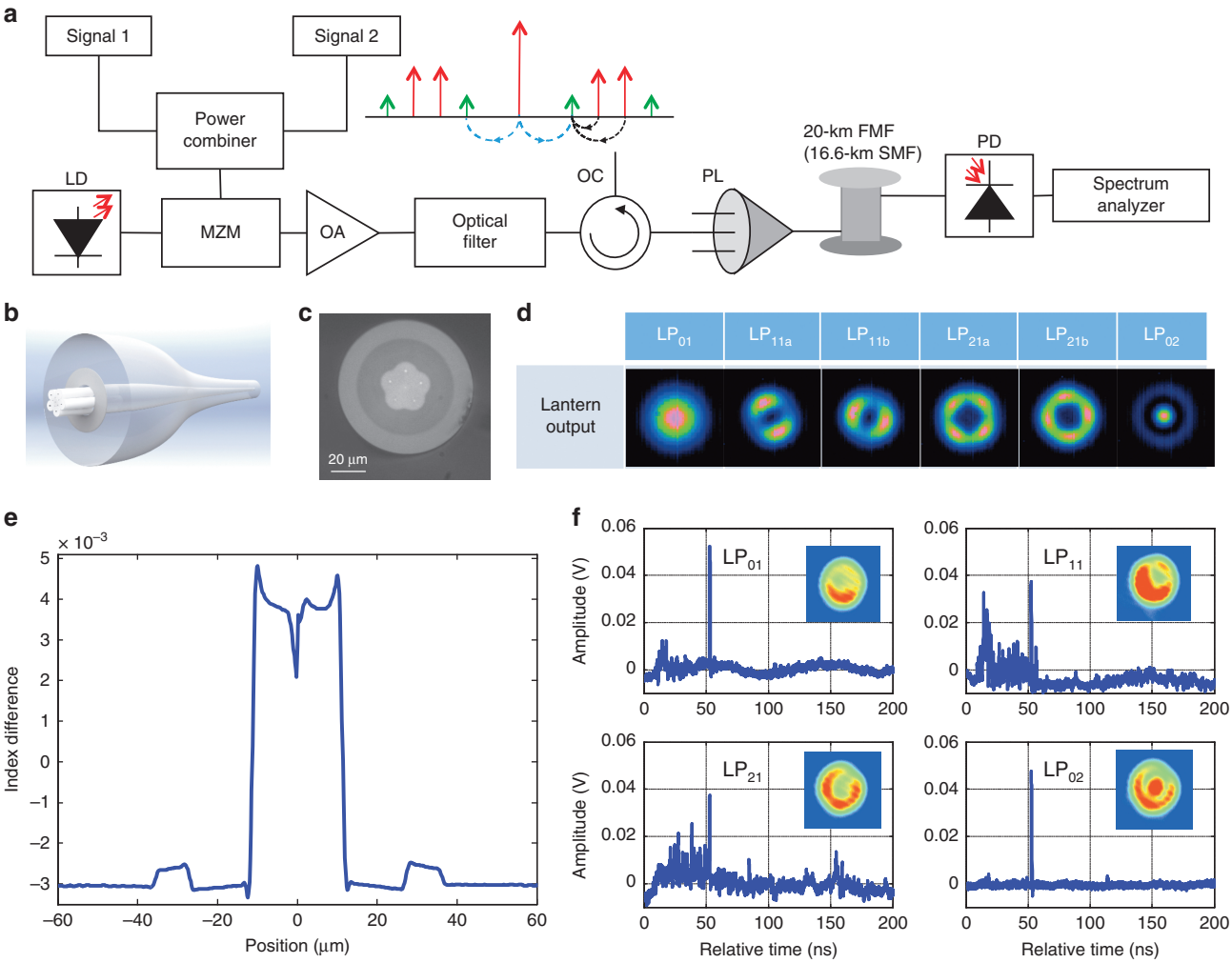

Figure 1 Single-channel microwave signal transmission over a FMF link. (**a**) Experimental setup. (**b**) Schematic of the PL. (**c**) Cross-sectional image of the PL output facet. (**d**) Output mode profiles of the PL. (**e**) Refractive-index profile of the FMF specially designed for single-channel transmission. (**f**) Impulse responses of the FMF excited by input mode LP_{01}, LP_{11}, LP_{21} and LP_{02}, respectively. Insets are output intensity profiles at the end of the FMF. LD, laser diode; MZM, Mach–Zehnder modulator; OA, optical amplifier; OC, optical circulator; PD, photodetector; PL, photonic lantern.

photodetection for the target signal carried on the LP_{01} mode. The input SMF of the filter was spliced directly to the FMF to receive the target signal. The residual optical power from the interfering channel was 34 dB down from the optical power in the target channel, leading to a background microwave signal crosstalk of less than −60 dB.

RESULTS AND DISCUSSION

Single-channel microwave signal transmission in FMFs

Figure 3 shows the performances of the FMF microwave photonic link, in comparison with a SMF microwave photonic link. For a fair comparison of nonlinear performances, the lengths of the FMF and SMF are set to 20 and 16.6 km, respectively, so that they have an identical effective nonlinear length. In Figure 3a, the back-scattered and transmitted optical powers are plotted against normalized optical launch power under microwave modulation. This normalization equalizes the loss of these two links (see section 4 of Supplementary Information for justifications and detailed procedures) so that the two links produce the same power at the fundamental frequency for the same normalized optical launch power without fibre nonlinearity. The SBS threshold for the FMF is ~25 dBm, about 8.7 dB larger than that of SMF. The resulting transmitted optical power at the SBS threshold is also 8.7 dB higher for the FMF. Even though the transmitted optical power increases beyond the SBS threshold, the transmitted signal contains multi-path interference due to SBS, leading to severe degradations in the SNR[50,51]. So, the maximum useful transmitted optical power is at the SBS threshold. The reason why the transmitted power still increases beyond the SBS threshold is because the power in the optical carrier is transferred to the sidebands through the Kerr effect, including SPM and FWM. Although the power of the optical carrier stops increasing due to SBS, the power of sidebands will grow if they are below the SBS threshold. As a result, the total transmitted optical power continues to increase but at a slower rate than below the SBS threshold. This is different from the CW case[50,51], where the transmitted power stops increasing beyond SBS threshold. Based on the effective areas of these two fibres, the SBS threshold for the FMF should be only 5.8 dB higher. An important factor for the additional increase in the SBS threshold is that the guided acoustic waves[52,53] have a smaller overlap with the high-order modes than with the fundamental mode (see section 5 of Supplementary Information), an advantage that can only be materialized in FMF fibres. In other words,

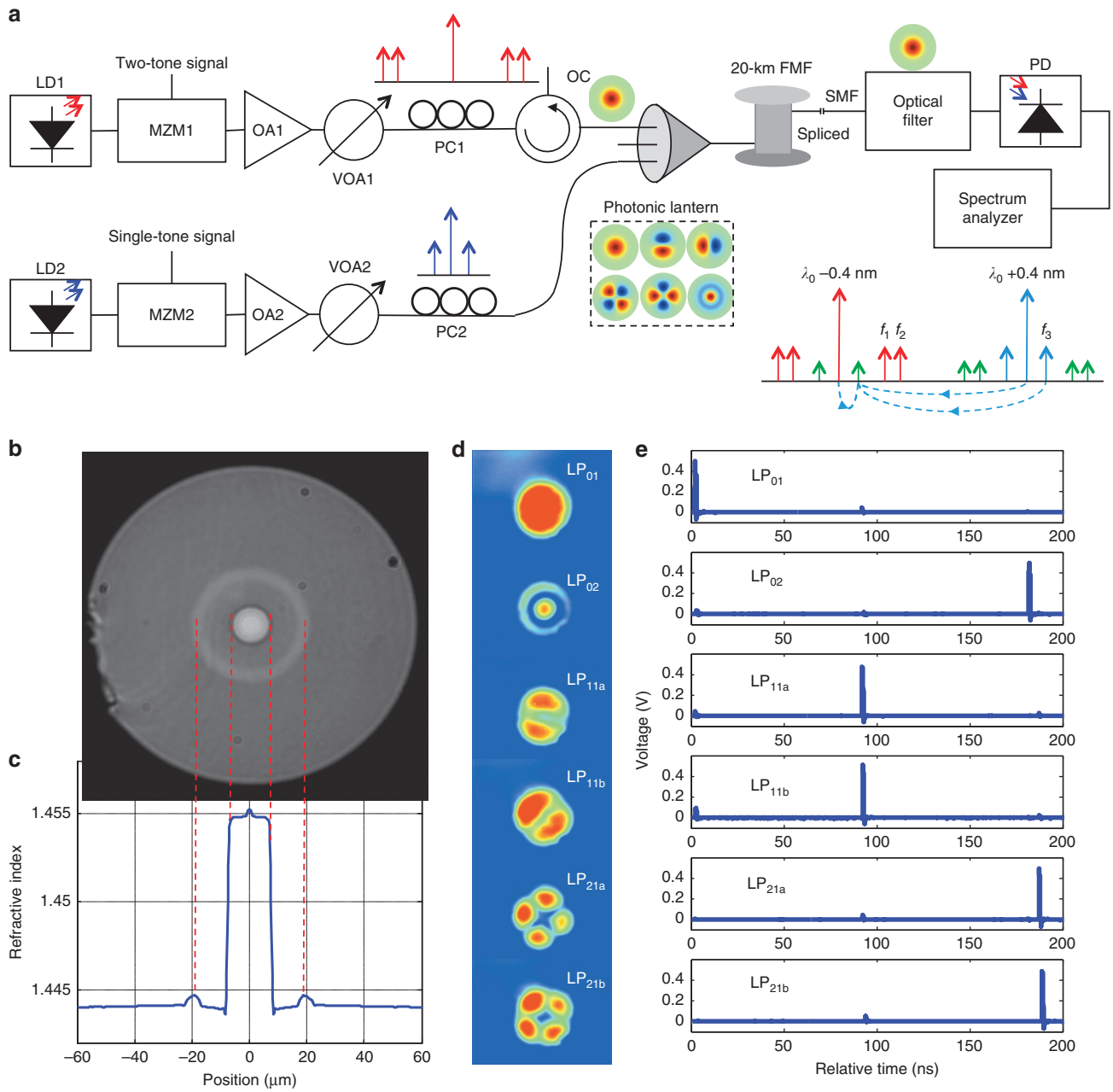

Figure 2 WDM transmission over a FMF link experiment. (**a**) Experimental setup. Two light waves with 100-GHz channel spacing are coupled into a FMF through a mode-selective photonic lantern. The target channel at a longer wavelength is modulated by two tones and launched into the LP_{01} mode. The interfering channel is modulated by a single tone and launched into one of the four mode groups: LP_{01}, LP_{11}, LP_{21} and LP_{02}. The inset illustrates the generation of nonlinear crosstalk due to four-wave mixing. (**b**,**c**) Cross-sectional image and refractive-index profile of the 6-mode FMF. (**d**) Output mode intensity profiles after transmission through the FMF. (**e**) Impulse response of the FMF excited by different input modes. LD, laser diode; MZM, Mach–Zehnder modulator; OA, optical amplifier; OC, optical circulator; PC, polarization controller; PD, photodetector; VOA, variable optical attenuator.

high-order modes have smaller acousto-optic effective areas[54,55] than the fundamental mode. Back reflection from the interface between the photonic lantern and the FMF may also lead to a slight overestimation of the SBS threshold.

The 8.7-dB increase in maximum transmitted optical power at the SBS threshold for the FMF leads to a 17.0-dB increase in detected microwave power or, equivalently, a 17.0-dB increase in the link gain as shown in Figure 3b. Even if we assume the launch power for the SMF could be increased to the SBS threshold for the FMF, the FMF link gain is still 6 dB higher than the SMF link. Increases in the gain can support longer transmission distances or larger splitting ratios.

The third-order intermodulation distortion (IMD3) also grows with the normalized optical launch power, as shown in Figure 3c. Different from the fundamental power, there is no deceleration of the IMD3 power beyond the SBS threshold. This is because the Kerr nonlinearity induces power transfer to IMD3. The optical spectral components that result in IMD3 include not only the optical carrier but also the modulation sidebands and FWM sidebands. As explained in section 6

doi:10.1038/lsa.2017.21

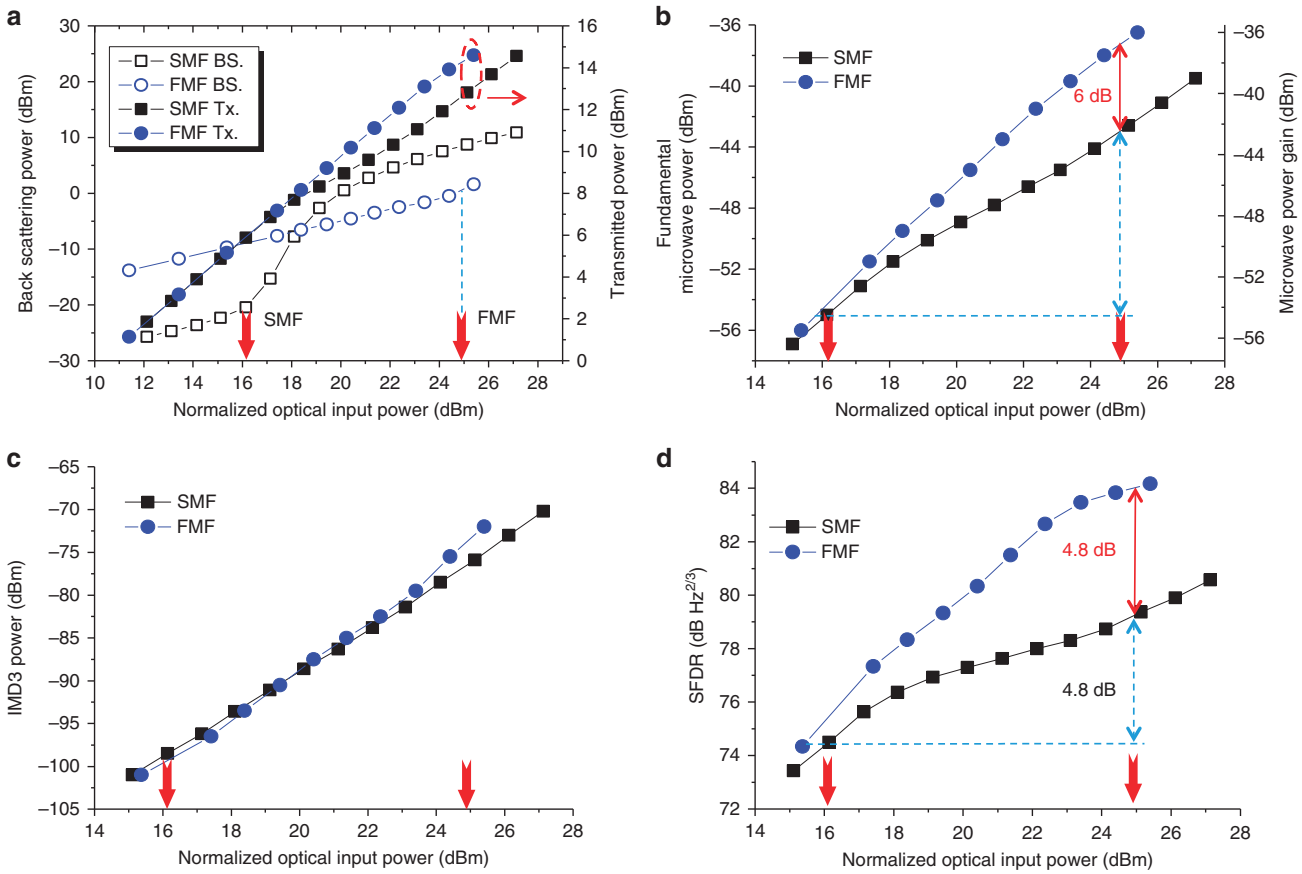

Figure 3 Experimental results of single-channel microwave signal transmission over a FMF link in comparison of over a SMF link. (**a**) Back-scattered (open symbols for the left axis) and transmitted (solid symbols for the right axis) optical power versus normalized optical launch power for FMF (circle) and SMF (square). Thick red arrows indicate the SBS thresholds of SMF and FMF. (**b**) Received microwave power at the fundamental frequency (left axis) and microwave power gain (right axis). (**c**) Third-order intermodulation distortion versus normalized optical launch power with microwave modulation power fixed at −0.5 dBm for each tone. The received microwave power at the fundamental frequency for the FMF link is 6 dB stronger than that of SMF link due to increased SBS threshold. (**d**) Spurious-free dynamic range versus normalized optical launch power. The FMF link provides a 9.6-dB improvement in SFDR.

of the Supplementary Information, the dominant contribution to the fundamental power comes from the optical carrier. As the optical carrier is depleted by the SBS, the fundamental power grows sub-linearly with the square of the launch power (slope of 1.3 on a log–log scale, smaller than the slope of 2 in the linear regime). In contrast, the dominant contribution to IMD3 comes from the modulation side-bands, which increase in power due to parametric amplification even beyond the SBS threshold. As a result, the IMD3 power still grows as a function of launch power at a slope of 2.5 on a log–log scale beyond the SBS threshold. It should be noted that, even though the effective area of the FMF is large and therefore the Kerr nonlinear coefficient is smaller, IMD3 in the FMF link is stronger at high launch powers, because the power in the optical carrier is stronger due to weaker SBS as compared to that in SMF.

As expected, the rate of increase in SFDR as a function of the normalized optical launch power, as shown in Figure 3d, will slow down once fibre nonlinearities set in. On one hand, the received microwave power at the fundamental frequencies will be suppressed due to SBS. Generally, a 1-dB reduction in fundamental power leads to 1-dB reduction in SFDR. On the other hand, FWM increases the IMD3. Generally, a 1-dB increase in IMD3 results in a 1/3-dB reduction in SFDR. Since the FMF has a higher SBS threshold than the SMF, the resulting SFDR of the FMF link is 4.8 dB higher than that of the SMF link at the SBS threshold of the FMF. The contributions of the microwave power at the fundamental frequency and IMD3 are 6 and −1.2 dB, respectively. However, analogue links should not operate above the SBS threshold as discussed before. So when compared at their respective SBS thresholds, the SFDR of the FMF link is 9.6 dB higher than that of the SMF link, where the contributions of the fundamental and IMD3 powers are 17.9 and −8.3 dB, respectively.

WDM microwave signal transmission in FMFs

Figure 4 compares the nonlinear crosstalk in WDM transmission with and without mode diversity versus received optical power. The difference for degenerated modes in the same mode group is small (see section 7 of Supplementary Information). As expected, a 1-dB increase in received optical power leads to a 3-dB rise in the nonlinear crosstalk, as shown in Figure 4a, in comparison with the 2-dB rise in IMD3. This is because the nonlinear crosstalk comes from the interaction of optical carrier of the target channel, and optical carrier and sidebands of the interfering channel, while IMD3 comes from the beating between the sidebands corresponding to the two tones, which is much weaker than the optical carrier. At moderate received optical powers, the nonlinear crosstalk easily surpasses the noise floor set by the photodetection process (−115 dB kHz^{-1} in our experiment). In this case, the noise floor that is normally used to define SFDR should

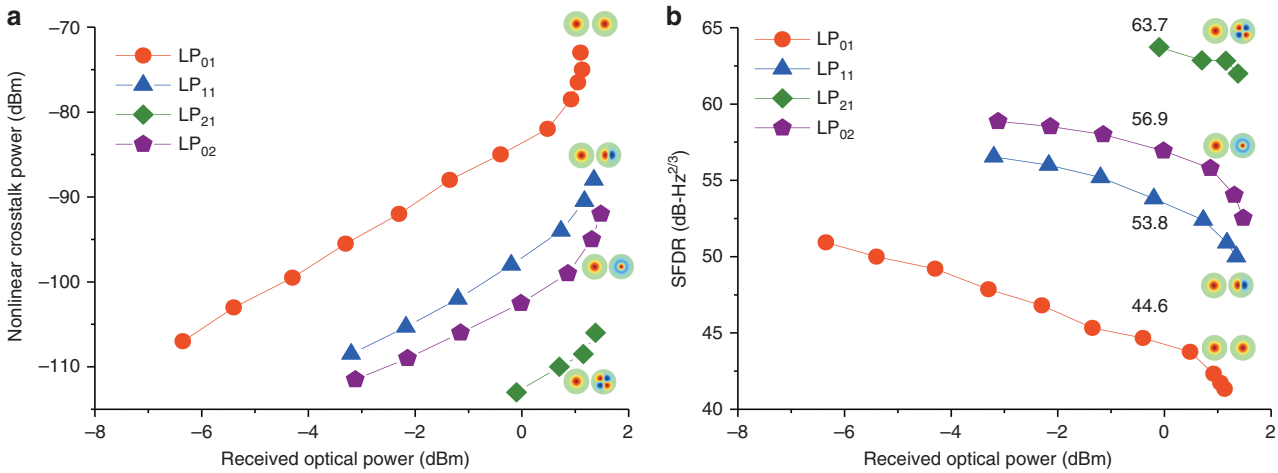

Figure 4 Experimental results on WDM transmission using mode diversity in comparison with WDM transmission using only the fundamental mode. (**a**) Detected microwave power due to nonlinear crosstalk coming from the interfering channel via fibre FWM effect. Mode-diversity configuration greatly suppresses nonlinear crosstalk using the orthogonality of different spatial modes. (**b**) Estimated SFDRs at the onset of nonlinear crosstalk.

be replaced by the nonlinear crosstalk (see section 8 of Supplementary Information). The reduction in SFDR due to nonlinear crosstalk can reach a few tens of dB as shown in Figure 4b. The values of 63.7, 56.9, 53.8 and 44.6 dB correspond SFDRs for each mode at the onset of FWM crosstalk (similarly defined to the SBS threshold). The most serious case is when both channels are in the LP_{01} mode. Using mode diversity, suppression of nonlinear crosstalk up to 30-dB, equivalent to a 20-dB increase in SFDR, was obtained. This level of nonlinear crosstalk suppression, although already very significant, was in fact much smaller than theoretically possible because the spatial orthogonality condition was not completely maintained due to linear crosstalk of the MSPL into the LP_{01} mode. As shown in Figure 3e, the LP_{21} mode has the least amount of mode crosstalk that results in the lowest nonlinear crosstalk.

Discussion

Further improvements in few-mode fibre-optic microwave photonic links rely on reducing the loss and crosstalk of the FMF link. Fortunately, it is expected that both the loss and crosstalk can be improved significantly from the links used in these experiments. In terms of losses, a few-mode fibre with loss as low as 0.16 dB km^{-1} has been demonstrated recently[56]. Fundamentally, the loss of FMFs should be comparable to that of traditional SMFs. Distributed mode crosstalk produced by the FMF itself can be reduced to negligible levels by increasing refractive-index difference and proper profile design[49]. Likewise, discrete mode crosstalk introduced by the mode multiplex can also be improved by optimizing the photonic lantern[57] or employing other multiplexing techniques such as the directional coupler[58] and the multi-plane light conversion[59].

The optimum number of modes for the FMF is indeed a critical parameter for WDM applications. In theory, if modes are truly orthogonal and free from crosstalk among each other, then the more modes we have, the more WDM channels can be accommodated in FMF transmission to avoid crosstalk. But in practice, linear crosstalk and fibre loss increases with the number of modes in the FMF and the mode multiplexers and demultiplexers. The optimum number of modes depends on technological progress in controlling crosstalk and loss. The employment of FMF can also mitigate other nonlinear distortions, in particular, second-order IMD for the transmission of multi-octave microwave signals.

It is also important to know at what length scale microwave photonic links should use FMFs instead of SMFs, especially in view of the potentially higher losses for FMF links. First, contrary to intuition, excess losses due to mode exciting devices such as the photonic lantern do not affect the link performance. This is because these losses can be easily compensated by increasing the optical power of the transmitting laser. Second, at short lengths, the maximum output power of the link will be predominantly determined by the nonlinear tolerance (the effective area) and not the loss of the fibre. So, FMFs will offer larger gains and dynamic ranges than SMFs (although for some applications, SMFs may be adequate). Third, at long distances, both fibre attenuation and effective area will affect the link performance since they determine how much power can be injected into the link and how much power actually arrives at the receiver. At long distances, FMF links will outperform SMF links if

$$P_{\mathrm{SBS}}^{\mathrm{FMF}}\left(\alpha_{\mathrm{FMF}}, A_{\mathrm{eff}}^{\mathrm{FMF}}, L\right) - \alpha_{\mathrm{FMF}} L \geq P_{\mathrm{SBS}}^{\mathrm{SMF}}\left(\alpha_{\mathrm{SMF}}, A_{\mathrm{eff}}^{\mathrm{SMF}}, L\right) - \alpha_{\mathrm{SMF}} L \quad (1)$$

where the SBS threshold for the FMF or SMF, $P_{\mathrm{SBS}}^{\mathrm{FMF}}$ or $P_{\mathrm{SBS}}^{\mathrm{SMF}}$, is a function of fibre attenuation coefficient α, effective area A_{eff} and fibre length L[27]. The left-hand and right-hand side of Equation (1) denotes the maximum output power without impairments from SBS for the FMF and SMF links, respectively. Using parameters of FMFs in this work, Equation (1) is satisfied for length up to 75 (45) km for the single-channel (WDM) transmission, respectively. Since the nonlinear length is shorter than 45 km, the best choice for long-distance links is to use FMFs at the beginning of the link where the optical power is the highest and then switch to low-loss SMFs past the nonlinear length of the FMF. Taking into account the three points above, we conclude that FMFs will lead to microwave photonic links with better performances regardless of the link length.

The spatial degrees of freedom have not been exploited for microwave photonics applications so far. We envision that few-mode microwave photonics can also offer other indispensable functionalities. For example, using few-mode components, we can generate large tunable delays based on modal dispersion[45] and realize wavelength-independent lossless signal combining as the performance of the MSPL can be made wavelength independent[60]. This work, therefore, represents the first step in the new field of few-mode microwave photonics.

doi:10.1038/lsa.2017.21

CONCLUSIONS

In this paper, we demonstrate order-of-magnitude improvement in dynamic range for both single-channel and WDM transmission of microwave signals. Without the single-mode constraint, FMFs can provide much larger effective areas than commercial single-mode, large effective-area fibres. Few-mode fibres also afford the opportunity to reduce the overlap between the guided acoustic and optical modes. Both of these factors increase the SBS threshold of FMFs. Significant increase in the SBS threshold and the nonlinear coefficient allow much larger optical powers to be launched and transported in the FMF. This work represents the first demonstration of using FMF to address the power-handling limitations of optical fibres for fibre-optic microwave photonic links. Furthermore, the introduction of the spatial degree of freedom into microwave signal transmission opens opportunities that cannot be afforded in single-mode fibres. Here we demonstrated suppression of nonlinear crosstalk by exploiting the orthogonality and walk-off of spatial modes.

CONFLICT OF INTEREST

The authors declare no conflict of interest.

ACKNOWLEDGEMENTS

This work is supported in part by the National Basic Research Program of China (973) Project #2014CB340104/3, NSFC Projects 61335005, 61377076, 61575142, 61431009 and 61671227, the United States Army Research Office grant W911NF-13-1-0283 and Shandong Provincial Natural Science Foundation (ZR2011FM015).

1 Capmany J, Novak D. Microwave photonics combines two worlds. *Nat Photonics* 2007; **1**: 319–330.
2 Cox CH, Ackerman EI, Betts GE, Prince JL. Limits on the performance of RF-over-fiber links and their impact on device design. *IEEE Trans Microwave Theory Tech* 2006; **54**: 906–920.
3 Seeds AJ, Williams KJ. Microwave photonics. *J Lightw Technol* 2006; **24**: 4628–4641.
4 Yao JP. Microwave photonics. *J Lightw Technol* 2009; **27**: 314–335.
5 Ackerman EI, Betts GE, Burns WK, Campbell JC, Cox CH *et al.* Signal-to-noise Performance of Two Analog Photonic Links Using Different Noise Reduction Techniques. 2007 IEEE/MTT-S International Microwave Symposium; 3–8 June 2007; Honolulu, HI, USA, pp. 51–54. IEEE: Honolulu, HI, USA, 2007.
6 Fiebig C, Blume G, Kaspari C, Feise D, Fricke J *et al.* 12 W high-brightness single-frequency DBR tapered diode laser. *Electron Lett* 2008; **44**: 1253–1255.
7 Ackerman EI. Broad-band linearization of a Mach-Zehnder electrooptic modulator. *IEEE Trans Microw Theory Tech* 1999; **47**: 2271–2279.
8 Howerton MM, Moeller RP, Greenblatt AS, Krahenbuhl R. Fully packaged, broad-band $LiNbO_3$ modulator with low drive voltage. *IEEE Photonics Technol Lett* 2000; **12**: 792–794.
9 Li GL, Yu PKL. Optical intensity modulators for digital and analog applications. *J Lightw Technol* 2003; **21**: 2010–2030.
10 Ishibashi T, Kodama S, Shimizu N, Furuta T. High-speed response of uni-traveling-carrier photodiodes. *Jpn J Appl Phys* 1997; **36**: 6263–6268.
11 Xie XJ, Zhou QG, Li KJ, Shen Y, Li QL *et al.* Improved power conversion efficiency in high-performance photodiodes by flip-chip bonding on diamond. *Optica* 2014; **1**: 429–435.
12 Urick VJ, Rogge MS, Bucholtz F, Williams KJ. Wideband (0.045–6.25 GHz) 40 km analogue fibre-optic link with ultra-high (>40 dB) all-photonic gain. *Electron Lett* 2006; **42**: 552–553.
13 Chen ZY, Yan LS, Pan W, Luo B, Zou XH *et al.* SFDR enhancement in analog photonic links by simultaneous compensation for dispersion and nonlinearity. *Opt Express* 2013; **21**: 20999–21009.
14 McKinney JD, Godinez M, Urick VJ, Thaniyavarn S, Charczenko W *et al.* Sub-10-dB noise figure in a multiple-GHz analog optical link. *IEEE Photonics Technol Lett* 2007; **19**: 465–467.
15 Cox III CH. *Analog Optical Links: Theory and Practice*. Cambridge: Cambridge University Press; 2004.
16 Rumelhard C, Algani C, Billabert AL. *Microwaves Photonic Links: Components and Circuits*. Hoboken, NJ: John Wiley & Sons; 2013.
17 Urick VJ, Williams KJ, McKinney JD. *Fundamentals of Microwave Photonics*. Chichester: John Wiley & Sons; 2015.
18 Urick VJ, Bucholtz F, McKinney J, Devgan PS, Campillo AL *et al.* Long-haul analog photonics. *J Lightw Technol* 2011; **29**: 1182–1205.
19 Ippen EP, Stolen RH. Stimulated Brillouin scattering in optical fibers. *Appl Phys Lett* 1972; **21**: 539–541.
20 Smith RG. Optical power handling capacity of low loss optical fibers as determined by stimulated Raman and Brillouin scattering. *Appl Opt* 1972; **11**: 2489–2494.
21 Stolen RH, Lin C. Self-phase-modulation *in silica* optical fibers. *Phys Rev A* 1978; **17**: 1448–1453.
22 Hill KO, Johnson DC, Kawasaki BS, MacDonald RI. cw three-wave mixing in single-mode optical fibers. *J Appl Phys* 1978; **49**: 5098–5106.
23 Chraplyvy AR. Limitations on lightwave communications imposed by optical-fiber nonlinearities. *J Lightw Technol* 1990; **8**: 1548–1557.
24 Horowitz M, Chraplyvy AR, Tkach RW, Zyskind JL. Broad-band transmitted intensity noise induced by Stokes and anti-Stokes Brillouin scattering in single-mode fibers. *IEEE Photonics Technol Lett* 1997; **9**: 124–126.
25 David A, Horowitz M. Low-frequency transmitted intensity noise induced by stimulated Brillouin scattering in optical fibers. *Opt Express* 2011; **19**: 11792–11803.
26 Le Bras H, Moignard M, Charbonnier B. Brillouin Scattering in Radio Over Fiber Transmission. Optical Fiber Communication Conference and Exposition and The National Fiber Optic Engineers Conference, pp. JWA86. Optical Society of America: Anaheim, CA, 2007.
27 Kobyakov A, Sauer M, Chowdhury D. Stimulated Brillouin scattering in optical fibers. *Adv Opt Photonics* 2010; **2**: 1–59.
28 Islam MN, Simpson JR, Shang HT, Mollenauer LF, Stolen RH. Cross-phase modulation in optical fibers. *Opt Lett* 1987; **12**: 625–627.
29 Payne J, Shillue B, Vaccari A. Photonic Techniques for Use on the Atacama Large Millimeter Array. International Topical Meeting on Microwave Photonics. Melbourne, Victoria: IEEE. 1999, pp. 105–108.
30 Wootten A, Thompson AR. The Atacama large millimeter/submillimeter array. *Proc IEEE* 2009; **97**: 1463–1471.
31 Ng W, Walston AA, Tangonan GL, Lee JJ, Newberg IL *et al.* The first demonstration of an optically steered microwave phased array antenna using true-time-delay. *J Lightw Technol* 1991; **9**: 1124–1131.
32 Goutzoulis AP, Zomp JM. Development and field demonstration of an eight-element receive wavelength-multiplexed true-time-delay steering system. *Appl Opt* 1997; **36**: 7315–7326.
33 Capmany J, Ortega B, Pastor D. A tutorial on microwave photonic filters. *J Lightw Technol* 2006; **24**: 201–229.
34 Liao JX, Xue XX, Wen H, Li SY, Zheng XP *et al.* A spurious frequencies suppression method for optical frequency comb based microwave photonic filter. *Laser Photonics Rev* 2013; **7**: L34–L38.
35 Urick VJ, Knapp PF, Swingen L, Rogge MS, Campillo AL *et al. Design and Characterization of Long-Haul Single-Channel Intensity-Modulated Analog Fiber-Optic Links*. Washington, DC: Naval Research Lab; 2005.
36 Urick VJ, Hastings A, Dexter JL, Williams KJ, Sunderman C *et al. Field Test on the Feasibility of Remoting HF Antenna with Fiber Optics*. Washington, DC: Naval Research Lab; 2008.
37 Wen H, Zheng HJ, Mo Q, Velázquez-Benitez AM, Xia C *et al.* Analog Fiber-Optic Links Using High-Order Fiber Modes. 2015 European Conference on Optical Communication (ECOC); 27 September–1 October 2015; Valencia, pp. 1-3. IEEE: Valencia, 2015.
38 Wen H, Mo Q, Sillard P, Amezcua Correa R, Li GF. Analog Transmission Over Few-Mode Fibers. Optical Fiber Communication Conference, pp. Th4A.3. Optical Society of America: Anaheim, CA, USA, 2016.
39 Urick VJ. Long-Haul Analog Links Tutorial. 2010 Conference on Optical Fiber Communication (OFC), Collocated National Fiber Optic Engineers Conference; 21–25 March 2010; San Diego, CA, USA. IEEE: San Diego, CA, USA, 2010.
40 Montebugnoli S, Boschi M, Perini F, Faccin P, Brunori G *et al.* Large antenna array remoting using radio-over-fiber techniques for radio astronomical application. *Microw Opt Technol Lett* 2005; **46**: 48–54.
41 Sauer M, Kobyakov A, George J. Radio over fiber for picocellular network architectures. *J Lightw Technol* 2007; **25**: 3301–3320.
42 Farwell ML, Chang WSC, Huber DR. Increased linear dynamic range by low biasing the Mach-Zehnder modulator. *IEEE Photonics Technol Lett* 1993; **5**: 779–782.
43 Leon-Saval SG, Fontaine NK, Salazar-Gil JR, Ercan B, Ryf R *et al.* Mode-selective photonic lanterns for space-division multiplexing. *Opt Express* 2014; **22**: 1036–1044.
44 Ramachandran S, Nicholson JW, Ghalmi S, Yan MF, Wisk P *et al.* Light propagation with ultralarge modal areas in optical fibers. *Opt Lett* 2006; **31**: 1797–1799.
45 Gasulla I, Capmany J. Microwave photonics applications of multicore fibers. *IEEE Photonics J* 2012; **4**: 877–888.
46 Essiambre RJ, Mestre MA, Ryf R, Gnauck AH, Tkach RW *et al.* Experimental investigation of inter-modal four-wave mixing in few-mode fibers. *IEEE Photonics Technol Lett* 2013; **25**: 539–542.
47 Xiao YZ, Essiambre RJ, Desgroseilliers M, Tulino AM, Ryf R *et al.* Theory of intermodal four-wave mixing with random linear mode coupling in few-mode fibers. *Opt Express* 2014; **22**: 32039–32059.
48 Sillard P, Astruc M, Boivin D, Maerten H, Provost L. Few-Mode Fiber for Uncoupled Mode-Division Multiplexing Transmissions. 37th European Conference and Exposition on Optical Communications; 18–22 September 2011; Geneva, pp. Tu.5.LeCervin.7. Optical Society of America: Geneva, 2011.
49 Maruyama R, Kuwaki N, Matsuo S, Ohashi M. Experimental Investigation of Relation Between Mode-Coupling and Fiber Characteristics in Few-Mode Fibers. Optical Fiber Communication Conference, pp. M2C.1. Optical Society of America: Los Angeles, CA, USA, 2015.
50 Fishman DA, Nagel JA. Degradations due to stimulated Brillouin scattering in multi-gigabit intensity-modulated fiber-optic systems. *J Lightw Technol* 1993; **11**: 1721–1728.

51 Ruffin AB. Stimulated Brillouin Scattering: an Overview of Measurements, System Impairments, and Applications. Technical Digest: Symposium on Optical Fiber Measurements; 28–30 September 2004; Boulder, CO, USA, pp. 23-28. IEEE: Boulder, CO, USA, 2004.
52 Shelby RM, Levenson MD, Bayer PW. Guided acoustic-wave Brillouin scattering. *Phys Rev B* 1985; **31**: 5244–5252.
53 Waldron RA. Some problems in the theory of guided microsonic waves. *IEEE Trans Microw Theory Tech* 1969; **17**: 893–904.
54 Ruffin AB, Li MJ, Chen X, Kobyakov A, Annunziata F. Brillouin gain analysis for fibers with different refractive indices. *Opt Lett* 2005; **30**: 3123–3125.
55 Kobyakov A, Kumar S, Chowdhury DQ, Ruffin AB, Sauer M *et al.* Design concept for optical fibers with enhanced SBS threshold. *Opt Express* 2005; **13**: 5338–5346.
56 Hayashi T, Tamura Y, Hasegawa T, Taru T. 125-μm-Cladding Coupled Multi-Core Fiber with Ultra-Low Loss of 0.158 dB/km and Record-Low Spatial Mode Dispersion of 6.1 ps/km$^{1/2}$. Optical Fiber Communication Conference Postdeadline Papers, pp. Th5A.1. Optical Society of America: Anaheim, CA, 2016.
57 Huang B, Fontaine NK, Ryf R, Guan BB, Leon-Saval SG *et al.* All-fiber mode-group-selective photonic lantern using graded-index multimode fibers. *Opt Express* 2015; **23**: 224–234.
58 Huang B, Xia C, Matz G, Bai N, Li GF. Structured Directional Coupler Pair for Multiplexing of Degenerate Modes. Optical Fiber Communication Conference/National Fiber Optic Engineers Conference 2013, pp. JW2A.25. Optical Society of America: Anaheim, CA, 2013.
59 Labroille G, Denolle B, Jian P, Genevaux P, Treps N *et al.* Efficient and mode selective spatial mode multiplexer based on multi-plane light conversion. *Opt Express* 2014; **22**: 15599–15607.
60 Xia C, Chand N, Velázquez-Benitez AM, Liu X, Lopez JEA *et al.* Demonstration of World's First Few-Mode GPON. 2014 The European Conference on Optical Communication (ECOC); 21–25 September 2014; Cannes, pp. 1-3. IEEE: Cannes, 2014.

This work is licensed under a Creative Commons Attribution-NonCommercial-ShareAlike 4.0 International License. The images or other third party material in this article are included in the article's Creative Commons license, unless indicated otherwise in the credit line; if the material is not included under the Creative Commons license, users will need to obtain permission from the license holder to reproduce the material. To view a copy of this license, visit http://creativecommons.org/licenses/by-nc-sa/4.0/

© The Author(s) 2017

Supplementary Information for this article can be found on the *Light: Science & Applications*' website (http://www.nature.com/lsa).